First-principles study of the impact of hydrogen passivation on the charge state transition levels of the $C_iO_i(Si_i)_n$ defect complexes in silicon

Abdulgaffar Abdurrazaq[a,c] · **Abdulrafiu T. Raji**[b] · **Walter E. Meyer**[a].

Abstract Density functional theory (DFT) with the Heyd-Scuseria-Ernzerhof hybrid functional, was used to predict the stability, formation energy, geometric structure, and the charge state transition levels of the $C_iO_i(Si_i)_n$ defect complex in silicon for $n = 0$, 1, 2. The effect of hydrogen passivation on the properties of the $C_iO_i(Si_i)_n$ defect complex was also investigated. The results for the binding energies confirm the stability of the defect complexes at neutral charge state. The charge state transition levels showed that C_iO_i induced a shallow donor level, and a deep acceptor level. The $C_iO_iSi_i$ and the $C_iO_i(Si_i)_2$ induced deep donor levels. After hydrogen passivation the acceptor level of the $C_iO_iSi_i$ and the $C_iO_i(Si_i)_i$ defect complexes disappeared and the donor levels for all the defect complexes moved deeper in the band gap.

Keywords Formation energy · Defect complexes · Charge states · Binding energy · Defect level

1 Introduction

Silicon (Si) has been used for applications in microelectronic, photovoltaic, and sensor devices [1]. As a result, silicon has become one of the most widely studied materials both experimentally and theoretically. Despite the development of new semiconductor materials, silicon is still the most common material used in electronic industries [2]. Therefore, it is important to improve silicon devices

[a]Department of Physics, University of Pretoria, Pretoria 0002, South Africa.
Tel.: +27630784509
· E-mail: a.abdurraza@up.ac.za
· [b]School of Interdisciplinary and Graduate Studies (SIRCGS), University of South Africa (UNISA), Mucklenuek, Pretoria 0003, South Africa.
E-mail: tunderaji@gmail.com
· [c]Ibrahim Shehu Shema Centre For Renewable Energy Research, Umaru Musa Yar'adua University, Dutsin-ma Road P.M.B. 2218 Katsina, Nigeria

and allow their use in to new applications by understanding the limitations of silicon at a fundamental level [3]. Carbon and oxygen are common impurities in silicon grown by different methods [4]. Therefore the understanding of oxygen and carbon- related defects is necessary in order to address the different technological challenges, particularly the limitations in fabrication [5], [6], [7], [8], [9], [10], [11], [12]. In radiation-damaged Czochralski (Cz) silicon, carbon and oxygen combine to form the C_iO_i defect complex, also called the C3 defect [13], [3]. For higher irradiation doses, the $C_iO_iSi_i$, known as the C4 center, is formed and even complexes of the form $C_iO_i(Si_i)_2$ have been observed [10], [14], [15], [15], [16]. In the last couple of years, advances in theoretical techniques and computational hardware have made it possible to model the electronic structure of point defects in semiconductors to an acceptable level of accuracy. For example the C_iO_i defect which was reported to have a measured donor level (+1/0) at E_V + 0.38 eV [17] was modelled by Backlund *et al.* [18] using the local density approximation (LDA) predicting a donor level at E_V + 0.3 eV. Using the same LDA functional, a donor level at E_V + 0.74 eV, was reported for the $C_iO_iSi_i$ defect complex [18]. It was reported that in all silicon fabrication processes, the hydrogen impurity is always found at the interstitial sites, and can diffuse very fast to bind to native point defects thereby eliminating their electrical activity or induce electrical activity in other defect complexes [19]. Recently measured transient capacitance data was used to characterizee clean silicon surface state and copper contaminated silicon surfaces [20]. Hydrogen was found to passivate both the clean and copper contaminated state [21]. Similarly hydrogen was also found to passivate carbon-oxygen related defect complexes in Cz silicon [22]

The charge state transition levels of a defect are important parameters describing its behaviour and approximately correspond to deep-level transient spectroscopy (DLTS) levels. Since both the generalised gradient approximation (GGA) and the local density approximation (LDA) wrongly predict the band gap of semiconductors, and the Heyd-Scuseria-Ernzerhof (HSE) functional is able to do so [23], [24], we decided to model the defect levels of the C_iO_i, $C_iO_iSi_i$, and the $C_iO_i(Si_i)_2$ defect complexes, together with the hydrogen passivated defects $C_iO_iH_i$, $C_iO_iSi_iH_i$, and the $C_iO_i(Si_i)_2H_i$.

2 Computational details

The QUANTUM ESPRESSO software package [25], with norm-conserving pseudopotentials [26], [27], was used to perform the density functional theory (DFT) calculations using the Heyd-Scuseria-Ernzerhof (HSE) functional [28], [29]. The formation energy of a defect was calculated as described by ref [30], [31], [32], [33]:

$$E^f(defect,q) = E(defect,q) - E(pristine) + \sum_l (\Delta n)_l \mu_l + q[E_V + \varepsilon_F] + E^q_{Cor}, \quad (1)$$

where q is the charge of the supercell containing the defect, $E(pristine)$, is the energy of the supercell without the defect, μ_l is the chemical potential of atom l added or removed from the defect, E_{V} is the energy of the valence band, and ε_F is the Fermi level relative to the valence band. For charged supercells the electrostatic corrections E^q_{Cor} were computed using the Corrections For Formation Energy and Eigenvalues for charged defect simulations (CoFFEE) package [34]. The dielectric constant of silicon used in the correction was taken from ref [35]. The binding energy is the difference between the energy of the defect complex and its separate non-interacting constituent defects which is given by [36] [33]:

$$E_b = \sum_l E^f_{isolated} - E^f_{defect-complex}, \tag{2}$$

where $\sum_l E^f_{isolated}$ represents the summation of the formation energies of the isolated defects, and $E^f_{defect-complex}$ is the formation energy of the defect complex. The charge state transition level is the Fermi energy where the energies of formation of two charge states are equal and is given by [37][33]

$$\epsilon(q/q') = \frac{E^f(defect, q; \varepsilon_F = 0) - E^f(defect, q'; \varepsilon_F = 0)}{q' - q}. \tag{3}$$

Following a convergence test, all calculations were done using a 216-atom supercell, a $2 \times 2 \times 2$ Monkhorst-Pack [38] grid of k-points, and a 45 Ry energy cut-off. The Perdew-Burke-Ernzerhof (PBE) GGA functional was used to determine the effect of supercell cell size by calculating the formation energies of the neutral $C_iO_i(Si_i)_2$ defect complex using 64, 216, and 512-atom silicon supercells with a $3 \times 3 \times 3$, $2 \times 2 \times 2$ and $1 \times 1 \times 1$ Monkhorst-Pack [38] grid of k-points, respectively. The energy cut-off was 45 Ry. The difference in the formation energies between the 512-atom supercell and 216-atom supercell was less than 0.01 eV. It was decided that the increase in accuracy provided by the 512-atom supercell was not worth the additional computational expense. The convergence test with respect to the cut-off energy was performed using a 216-atom supercell and a $2 \times 2 \times 2$ Monkhorst-Pack [38] grid of k-points. When varying the cut-off energy from 45 Ry to 90 Ry, the total energy per atom only changed by 0.1 meV. The difference in minimum energy between the $3 \times 3 \times 3$ and $2 \times 2 \times 2$ k-point mesh was also less than 0.1 meV per atom.

Using these parameters, a pristine silicon supercell was constructed and fully relaxed using the PBE functional. Hereafter the HSE functional was used to determine the electronic structure from which a band gap of 1.18 eV was determined, which is in good agreement with the previous theoretical and experimental results [39] [40] [41]. The fully relaxed supercell using PBE was then modified to incorporate the defect under study. After this point, only atomic positions were relaxed keeping the dimensions of the cell constant. The supercells containing the defects were relaxed until the forces acting on each atom were less than 0.001 eV/Å and the difference in total energy between

the iterations was less than 10^{-5} eV. Then the HSE functional was used for all the electronic structure calculations.

3 Results and discussion

3.1 Structural properties

The relaxed structures of the defect complexes are shown in Fig. 1. Table 1 presents the predicted shortest bond length distances in Å between the silicon atoms and the introduced impurity atom. The stable structure as suggested by ref [3] was used for all the calculations. Typically, with atoms placed at their high symmetry positions, complexes involving H_i, C_i, O_i, and Si_i atoms relaxed significantly, with a decrease in bond length for the O_i and H_i versus an increase in bond length for the C_i and Si_i impurities. For a given species of atoms the bond lengths did not change significantly between the complexes.

3.2 Binding energy

Table 2 presents the computed binding energies for all the defect complexes. Here it can be seen that C_i and O_i can form a stable C_iO_i defect complex. Si_i can also bond strongly with C_iO_i to form the $C_iO_iSi_i$ defect complex. Another Si_i can readily bond to $C_iO_iSi_i$ to form a stable $C_iO_i(Si_i)_2$ defect complex. Our results also showed that H_i readily interacts with C_iO_i to form a stable $C_iO_iH_i$ defect complex. $C_iO_iSi_i$ also can readily interact with H_i to form a stable $C_iO_iSi_iH_i$ defect complex, and lastly H_i also binds to $C_iO_i(Si_i)_2$ to form a stable $C_iO_i(Si_i)_2H_i$ defect complex.

3.3 Thermodynamic transition energy levels

The charge state transition levels with respect to the energy of the valence band (E_V) of all the defect complexes are presented in Table 3. Fig. 2 shows the plot for the formation energy as a function of Fermi energy. There was good agreement between our results and the experimentally measured donor levels for the C_iO_i and the $C_iO_iH_i$ defect complexes, the only complexes for which the experimental results were available. For the C_iO_i, the results obtained from this study are closer to the experimental values than those obtained by using LDA calculations. The donor level of the $C_iO_iSi_i$ defect agreed reasonably well with a previous LDA calculation. For other defect levels there is no available experimental or theoretical data. For the defect $C_iO_iSi_i$ and $C_iO_i(Si_i)_2$ when compared to C_iO_i the donor level increased from 0.37 eV to 0.66 eV and 0.74 eV, moving towards the middle of the band gap.

Except for C_iO_i defect complex all donor levels of all the defect complexes shifted deeper to the conduction band after hydrogen passivation. While the shallower acceptor levels disappeared completely in to the conduction band.

4 Summary

Detailed calculations of the formation energies, binding energies, and the thermodynamic transition energy levels of $C_iO_i(Si_i)_n$ defect complexes before and after hydrogen passivation was carried out, using the hybrid density functional theory. The binding energies at zero charge state showed that H_i can readily interact with the $C_iO_i(Si_i)_n$ defect complexes to form the stable $C_iO_i(Si_i)_nH_i$ defects complexes. The predicted donor levels shifted towards the conduction band after hydrogen passivation. While the shallower acceptor levels disappeared after hydrogen passivation. The shallow double donor electronic levels also shift towards the conduction band making a deep double donor level after hydrogen passivation, except for the C_iO_i defect complex, where the shallow double donor level shift to the valence band. Agreement was found with the experimental donor levels of C_iO_i defect complex before and after hydrogen passivation. There is also an agreement for the donor level predicted by GGA calculations for the $C_iO_iSi_i$ defect complex, and no available experimental or theoretical values for the other defect complexes.

Table 1 The predicted bond length between the impurity atoms and the nearest Si atom before and after relaxation of the neutral defect. α_d, β_d, Δ_d, and θ are the bond length before relaxation, bond length after relaxation, the difference between the bond lengths before and after relaxation, and the bond angles after relaxation respectively. All distances are in Å, and all angles are in degrees.

Bonds	α_d	β_d	Δ_d	θ
O_i-Si	2.03	1.76	−0.27	89.0
	2.03	1.79	−0.24	140.4
	2.03	1.87	−0.16	132.0
C_i-Si	2.03	1.78	−0.25	140.5
	2.03	1.80	−0.23	125.0
	2.03	1.76	−0.27	93.0
H_i-Si	1.71	1.88	0.15	123.6
	1.71	1.85	0.14	120.3
	1.71	1.89	0.18	113.8
Si_i-Si	2.03	2.27	0.24	148.4
	2.03	2.28	0.25	145.5
	2.03	2.27	0.24	148.0

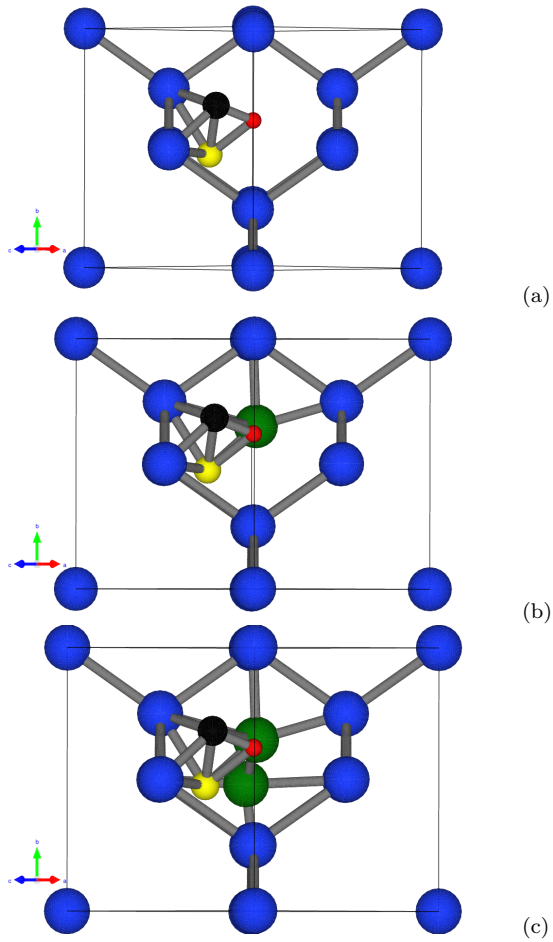

Fig. 1 The relaxed geometric structures for the (a) $C_iO_iH_i$, (b) $C_iO_iSi_iH_i$, and (c) $C_iO_i(Si_i)_2H_i$ defect complex. The blue balls represent silicon atoms, the green balls represent silicon self interstitial, the black balls represent carbon, the yellow balls represent oxygen, and the red balls represent hydrogen atoms.

Acknowledgements This work is based on the research supported partly by National Research foundation (NRF) of South Africa (Grant specific unique reference number (UID) 98961). The opinions, findings and conclusion expressed are those of the authors and the NRF accepts no liability whatsoever in this regard. The authors acknowledge the Center For High Performance Computing (CHPC) Cape Town, South Africa for computational resources.

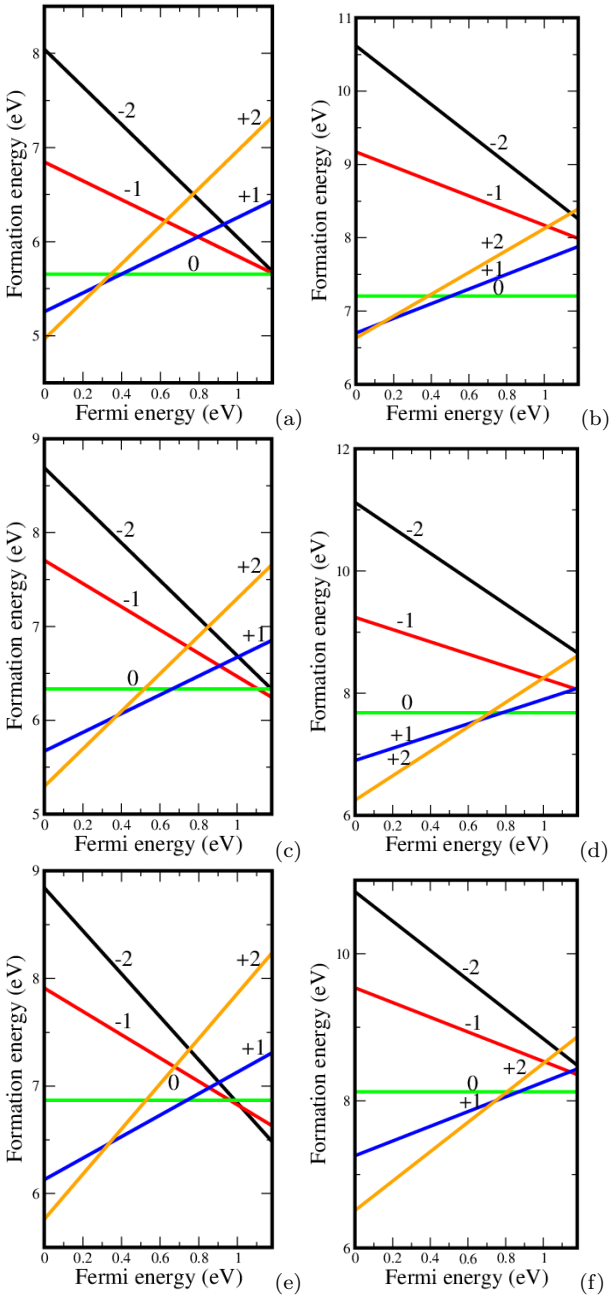

Fig. 2 The plots of the thermodynamic charge state transition energy levels for the (a)C_iO_i (b) $C_iO_iH_i$ (c) $C_iO_iSi_i$ (d) $C_iO_iSi_iH_i$ (e)$C_iO_i(Si_i)_2$ and (f) $C_iO_i(Si_i)_2H_i$ defect complexes.

Table 2 Binding energy E_b for the neutral charge state of the defect complexes in eV.

Defect	Reaction	E_b
C_iO_i	$C_i + O_i$	1.86
$C_iO_iH_i$	$C_iO_i + H_i$	0.48
$C_iO_iSi_i$	$C_iO_i + Si_i$	0.47
$C_iO_iSi_iH_i$	$C_iO_iSi_i + H_i$	0.28
$C_iO_i(Si_i)_2$	$C_iO_iSi_i + Si_i$	0.32
$C_iO_i(Si_i)_2H_i$	$C_iO_i(Si_i)_2 + H_i$	0.19

Table 3 The thermodynamic transition energy levels $\epsilon(q/q')$ with respect to the energy of the valence band E_V for the defect complexes.

Defect	Study	$(+2/+1)$	$(+1/0)$	$(0/-1)$
C_iO_i	This study	0.29	0.37	–
	LDA model [19]	–	0.30	–
	Experiment [18]	–	0.38	–
$C_iO_iH_i$	This study	0.18	0.52	–
	Experiment [42]	–	0.41	–
$C_iO_iSi_i$	This study	0.37	0.66	1.10
	LDA model [19]	–	0.74	–
$C_iO_iSi_iH_i$	This study	0.64	0.79	–
$C_iO_i(Si_i)_2$	This study	0.34	0.74	0.96
$C_iO_i(Si_i)_2H_i$	This study	0.77	0.86	–

References

1. H. Wang, A. Chroneos, C. Londos, E. Sgourou, U. Schwingenschlögl, Applied Physics Letters 103 (5) (2013) 052101.
2. C. Londos, E. Sgourou, D. Hall, A. Chroneos, Journal of Materials Science: Materials in Electronics 25 (6) (2014) 23952410.
3. S.-R. Christopoulos, E. Sgourou, T. Angeletos, R. Vovk, A. Chroneos, C. Londos, Journal of Materials Science: Materials in Electronics 28 (14) (2017) 1029510297.
4. J. Cautinho, R. Jones, P. Briddon, S. berg, L. Murin, V. Markevich, J. LindstrJm, Physical Review B 65 (1) (2001) 014109.
5. J. Coutinho, R. Jones, P. Briddon, S. berg, Physical Review B 62 (16) (2000) 10824.
6. C. Londos, A. Andrianakis, V. Emtsev, H. Ohyama, Semiconductor Science and Technology 24 (7) (2009) 075002.
7. A. Chroneos, C. Londos, E. Sgourou, P. Pochet, Applied Physics Letters 99 (24) (2011) 241901.
8. H. Wang, A. Chroneos, C. Londos, E. Sgourou, U. Schwingenschlgl, Scientific reports 4 (2014) 4909.
9. T. Angeletos, A. Chroneos, C. Londos, Journal of Applied Physics 119 (12) (2016) 125704.
10. C. Londos, M. Potsidi, E. Stakakis, Physica B: Condensed Matter 340 (2003) 551555.
11. A. Chroneos, E. Sgourou, C. Londos, U. Schwingenschlgl, Applied Physics Reviews 2 (2) (2015) 021306.
12. E. Sgourou, D. Timerkaeva, C. Londos, D. Aliprantis, A. Chroneos, D. Caliste, P. Pochet, Journal of Applied Physics 113 (11) (2013) 113506.
13. L. Murin, J. Lindstrm, G. Davies, V. Markevich, Nuclear Instruments and Methods in Physics Research Section B: Beam Interactions with Materials and Atoms 253 (1-2) (2006) 210213.
14. G. Davies, E. Lightowlers, R. Newman, A. Oates, Semiconductor science and technology 2 (8) (1987) 524.
15. M. Brozel, R. Newman, D. Totterdell, Journal of Physics C: Solid State Physics 8 (2) (1975) 243.

16. L. I. Murin, B. G. Svensson, V. P. Markevich, A. R. Peaker, in: Solid State Phenomena, Vol. 205, Trans Tech Publ, 2014, pp. 218223.
17. P. Mooney, L. Cheng, M. Sli, J. Gerson, J. Corbett, Physical Review B 15 (8) (1977) 3836.
18. D. Backlund, S. Estreicher, Physical Review B 77 (20) (2008) 205205.
19. C. G. Van de Walle, J. Neugebauer, Annu. Rev. Mater. Res. 36 (2006) 179198.
20. Song L , Xie M , Yu X . Appl. Phys. Lett. 111(15) (2017) 152103.
21. L. Song, D. Yang, X. Yu, AIP Advances 9 (2019) 105102
22. Abdurrazaq A, Meyer W E. Physica B: Condensed Matter, 2019, 572: 238-241
23. P. Deak, B. Aradi, T. Frauenheim, E. Janzen, A. Gali, Physical Review B 81 (15) (2010) 153203.
24. J. Kusima, J. Ojanen, J. Enkovara, T. Rantala, Physical Review B 82 (11) (2010) 115106.
25. P. Giannozzi, S. Baroni, N. Bonini, M. Calandra, R. Car, C. Cavazzoni, D. Ceresoli, G. L. Chiarotti,M. Cococcioni, I. Dabo, et al., Journal of physics: Condensed matter 21 (39) (2009) 395502.
26. C. Hartwigsen, S. Gdecker, J. Hutter, Physical Review B 58 (7) (1998) 3641.
27. S. Goedecker, M. Teter, J. Hutter, Physical Review B 54 (3) (1996) 1703.
28. J. Heyd, G. E. Scuseria, M. Ernzerhof, The Journal of chemical physics 118 (18) (2003) 82078215.
29. A. V. Krukau, O. A. Vydrov, A. F. Izmaylov, G. E. Scuseria, The Journal of chemical physics 125 (22) (2006) 224106.
30. C. Freysoldt, B. Grabowski, T. Hickel, J. Neugebauer, G. Kresse, A. Janotti, C. G. Van de Walle, Reviews of modern physics 86 (1) (2014) 253.
31. Y. Kumagai, F. Oba, Physical Review B 89 (19) (2014) 195205.
32. P. Haas, F. Tran, P. Blaha, Physical Review B 79 (20) (2009) 209902.
33. A. Abdurrazaq, W. Meyer, Physica B: Condensed Matter.
34. M. H. Naik, M. Jain, Computer Physics Communications 226 (2018) 114126.
35. J. Paier, M. Marsman, K. Hummer, G. Kresse, I. C. Gerber, J. G. ngyn, The Journal of chemical physics 124 (15) (2006) 154709.
36. G. Zollo, Y. Lee, R. Nieminen, Journal of Physics: Condensed Matter 16 (49) (2004) 8991.
37. C. Freysoldt, B. Grabowski, T. Hickel, J. Neugebauer, G. Kresse, A. Janotti, C. G. Van de Walle, Reviews of modern physics 86 (1) (2014) 253.
38. H. Monkhorst, J. Pack, Physical Review B 13 (1976) 5188.
39. J. Heyd, J. E. Peralta, G. E. Scuseria, R. L. Martin, The Journal of chemical physics 123 (17) (2005) 174101.
40. J. Paier, M. Marsman, K. Hummer, G. Kresse, I. C. Gerber, J. G. ngyn, The Journal of chemical physics 124 (15) (2006) 154709.
41. P. Haas, F. Tran, P. Blaha, Physical Review B 79 (20) (2009) 209902.
42. J. Coutinho, R. Jones, P. Briddon, S. berg, L. Murin, V. Markevich, J. LindstrJm, Physical Review B 65 (1) (2001) 014109.